

STELLACYANIN

Studies of the Metal-binding Site using X-ray Absorption Spectroscopy

J. PEISACH

*Departments of Molecular Pharmacology and Molecular Biology, Albert Einstein College of Medicine,
Bronx, New York 10461*

L. POWERS AND W. E. BLUMBERG

Bell Laboratories, Murray Hill, New Jersey 07974

B. CHANCE

*Johnson Research Foundation, University of Pennsylvania Medical School, Philadelphia, Pennsylvania
19104*

ABSTRACT Stellacyanin is a mucoprotein of molecular weight ~20,000 containing one copper atom in a blue or type I site. The metal ion can exist in both the Cu(II) and Cu(I) redox states. The metal binding site in plastocyanin, another blue copper protein, contains one cysteinyl, one methionyl, and two imidazolyl residues (Colman et al. 1978. *Nature [Lond.]*. 272:319–324.), but an exactly analogous site cannot exist in stellacyanin as it lacks methionine. The copper coordination in stellacyanin has been studied by x-ray edge absorption and extended x-ray absorption fine structure (EXAFS) analysis. A new, very conservative data analysis procedure has been introduced, which suggests that there are two nitrogen atoms in the first coordination shell of the oxidized [Cu(II)] protein and one in the reduced [Cu(I)] protein; these N atoms have normal Cu—N distances: 1.95–2.05 Å. In both redox states there are either one or two sulfur atoms coordinating the copper, the exact number being indeterminable from the present data. In the oxidized state the Cu—S distance is intermediate between the short bond found in plastocyanin and those found in near tetragonal copper model compounds. Above –140°C, radiation damage of the protein occurs. At room temperature the oxidized protein is modified in the x-ray beam at a rate of 0.25%/s.

INTRODUCTION

Ever since the original observation of their intense color, the blue copper proteins have been studied in order to understand the structure that gives rise to their unusual physical properties. Some of these properties include intense optical absorptions near 600 nm with molar extinction coefficients of 3,000–5,000 cm⁻¹, a nuclear hyperfine interaction in the EPR of 3–9 × 10⁻³ cm⁻¹, about one-quarter that of copper complexes having near tetragonal geometry, and oxidation-reduction potentials 100–600 mV higher than that for the Cu(II)/Cu(I) couple in aqueous solution (1,2).

Over the past decade, various structural explanations based on biochemical and spectroscopic evidence have been given for these properties that are related to the structural and stereochemical makeup of the copper binding site. For example, the intense blue color is believed to arise from a ligand-to-metal charge transfer from a cysteinyl sulfur (3,4). The EPR properties are thought to be due to the nontetragonal and likely near tetrahedral symmetry of the metal site (5), while the high redox potential is attributed to the stereochemical constraint that causes the

structure of the Cu metal-binding site in the oxidized protein to have a geometric array of ligands not very different from that of the reduced protein. In addition, NMR (6–8), electron spin echo (9,10), and ENDOR (electron-nuclear double resonance) (11) studies demonstrate that the metal binding site contains one or more imidazole nitrogen atoms, while the linear electric field effect in pulsed EPR (12) shows that the copper binding site has a large internal electric field, consistent with an accessible excited state charge-transfer interaction. Not all of these properties are reproduced by nonblue copper proteins, by model copper complexes made up of amino acids and peptides, or by model compounds of a more exotic nature (13,14).

A major breakthrough in our understanding of the blue copper proteins comes from the x-ray crystallographic analysis at 2.7-Å resolution and subsequent refinement to 1.6 Å of poplar leaf plastocyanin (15), a 10,500-dalton (D) molecule that contains a single copper atom. The extinction coefficient per copper atom for the analogous protein from *Chenopodium album* is 4,700 M⁻¹cm⁻¹ at 597 nm (16), while *A*₁, the nuclear hyperfine constant in the EPR for this protein (16) is 7.0 × 10⁻³ cm⁻¹. The redox potential

for bean plastocyanin is 347 mV (17). For the poplar protein in the oxidized state, the ligands to Cu(II) consist of two histidine imidazole nitrogen atoms and a cysteinyl sulfur. At a distance too far to constitute a real chemical bond (2.9 Å), another sulfur atom, from methionine, is found. A similar ligand arrangement is deduced for another low-molecular-weight, blue copper protein, azurin, in which the same atoms are arranged about the metal atom (18). Thus, many of the structural predictions based on spectroscopic measurements have been borne out. Others (19), regretfully, have not.

In addition to plastocyanin and azurin, a third blue copper protein that has drawn a great deal of attention since its discovery by Omura (20) is stellacyanin, a mucoprotein isolated from *Rhus vernicifera*, the Japanese lac tree (20,5). This 20,000-D molecule has physical properties that relegate it to the class of blue copper proteins, yet they are decidedly different from those of azurin and plastocyanin. To begin with, the redox potential of stellacyanin, 184 mV, is decidedly lower (17). The EPR spectrum of stellacyanin is indicative of rhombic symmetry (5,21), whereas those for azurin (22) and plastocyanin (16) indicate an axially symmetric site. A more fundamental difference is in the amino acid composition. Stellacyanin contains no methionine (5,23), which is a conserved near neighbor of copper in all azurins and plastocyanins. One finds a cysteinyl residue in the portion in stellacyanin said to be homologous with these methionine-containing regions (8). Although stellacyanin would be an attractive candidate for x-ray crystallographic study, the growth of a suitable crystal has proven to be an intractable problem, probably due to solubility properties which are in part governed by the large carbohydrate content of the molecule (5). For this reason, we have turned our attention to the EXAFS technique for the elucidation of the metal-binding site in this protein.

From the analysis of the data, we conclude that the ligands to the metal in oxidized stellacyanin are most probably two nitrogen atoms and one sulfur atom. The Cu—S bond length was determined to be ~ 2.21 Å, considerably larger (by at least 0.05 Å) than the analogous bond in plastocyanin and closer in distance to that found in the near planar CuN_2S_2 complex, Cu(II)-bis-thiosemicarbazone, (2.26 Å). There is no evidence for the presence of a methionyl sulfur analogue >2.5 Å away from the copper. There is, however, a ligand that may be sulfur at ~ 2.8 Å but that could also be nitrogen, carbon, or oxygen, or these in combination. In the case of reduced stellacyanin, one cannot unambiguously choose the correct mathematical solution from the analysis, but a first coordination shell consisting of one nitrogen and one sulfur atom provides the best fit to the data.

During the course of our studies, we found that stellacyanin protein easily became damaged by synchrotron radiation as demonstrated from changes in the EPR and optical properties of the oxidized protein. An analysis of

the EXAFS of this damaged material showed that the binding site for Cu(II) now consisted of two nitrogen and two sulfur atoms. In the reduced, radiation-damaged material, the ligands to Cu(I) are likely to be two nitrogen atoms and one or two sulfur atoms, 2.31–2.34 Å from the copper, which is a normal Cu(I)—S bond distance.

METHODS

Sample Preparation

Stellacyanin was prepared by the method of Mims and Peisach (9) from lac acetone powders purchased from Saito and Company (no. 9, Hommachi 1-Chome, Higashi-Ku, Osaka, Japan). After the last column chromatographic step, those fractions with an $A_{604}/A_{280} > 0.14$ were combined. The protein was concentrated under pressure (Amicon Corp., Scientific Systems Div., Lexington, MA) and equilibrated against 0.05 M KPO₄ buffer, pH 7. It was sometimes found that our stellacyanin preparations were only slowly reduced with dithionite, as judged from loss of blue color. We could, however, reduce the protein by using long-term anaerobic incubation with a large excess of dithionite.

Monitoring

To ensure protein integrity and redox state, optical spectroscopy was used to monitor the sample before, during, and after exposure to the x-ray beam. The samples were maintained at -140°C or lower to prevent damage by hydrated electrons and free radicals produced during exposure (24). However, in the case shown in Fig. 8, a temperature of -50°C was used to demonstrate optical bleaching. In addition, EPR measurements were made before and after each 10 min of x-ray exposure. The specifically designed optical spectrophotometer, sample holders, and EPR spectrometer used in this study are described elsewhere (25).

Measurements

All x-ray absorption measurements were made at Stanford Synchrotron Radiation Laboratory during dedicated operation of the SPEAR storage ring at 40–80 mA and ~ 3.0 GeV. Beamline I-5 was used exclusively for both edge and EXAFS measurements providing $\sim 1 \times 10^{10}$ photons/s.

The initial intensity was monitored by an ionization chamber preceded by a defining slit. The fluorescence was measured using the filter-fast plastic scintillator assembly described by Powers et al. (25). The samples, prepared in holders suitable for the cryostat (24,25), were maintained at -140°C or lower at all times.

Edge Spectra

Edge spectra were analyzed using the methods described previously (26). The error in absolute energy is ± 0.1 eV. The EXAFS data (Fig. 1) were analyzed by the methods described by Lee et al. (27) and Powers (28).

EXAFS Spectra

The modulation of the x-ray absorption spectrum by the EXAFS is given by

$$\chi(k) = \sum_i \frac{N_i}{k r_i^2} |f_i(k, \pi)|^2 (e^{-2k^2 \sigma_i^2 - \eta_i/\lambda}) \sin[2[kr_i + \alpha_i(k)]],$$

where the sum is over the distances r_i from the absorbing atom, N_i is the number of the same type of backscattering atoms at r_i , λ is the photoelectron mean free path and $f_i(k, \pi)$ is the backscattering amplitude of the i th atom which is $\sim Z/k^2$ (for atomic number Z) when $k > \sim 4 \text{ Å}^{-1}$. The disorder parameter σ^2 (sometimes called the Debye-Waller factor) describes the mean-square displacement in r_i that arises from thermal and/or lattice disorder. The phase shift $\alpha(k)$ is the energy-dependent

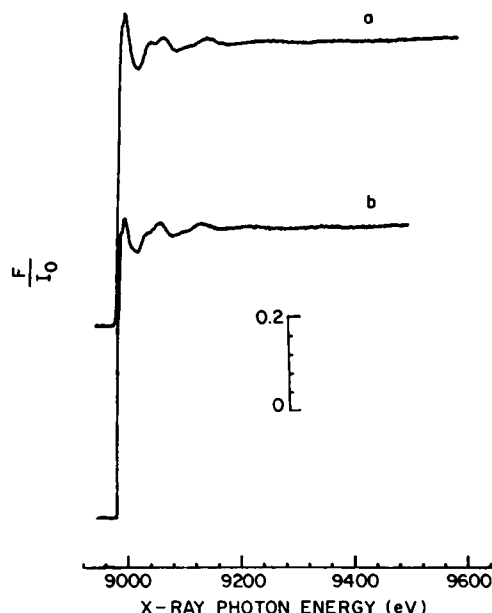


FIGURE 1 X-ray absorption spectra of (a) oxidized and (b) reduced stellacyanin at -140°C . A linear background that sets the absorption below the edge equal to zero has been removed.

phase resulting from the potentials of both the absorbing and backscattering atom, and k is the wave vector given by

$$k = (2 m_e [E - E_0])^{1/2} / \hbar$$

where m_e is the electron mass, E is the x-ray photon energy, and E_0 is the edge or threshold energy. Fig. 2 shows the $k^3\chi(k)$ data for both oxidized and reduced stellacyanin. These data were Fourier transformed without smoothing or use of a filter function and are shown in Fig. 3. Using a Fourier filter, each resolved shell was back-transformed (Fig. 4) and resolved into an amplitude and a phase function.

Model compounds for Cu—N and Cu—S amplitudes and phases for first coordination shells were Cu(II)-tetraphenylporphine (CuTPP), which has four nitrogen atoms at an average distance of 1.984 \AA (29), and

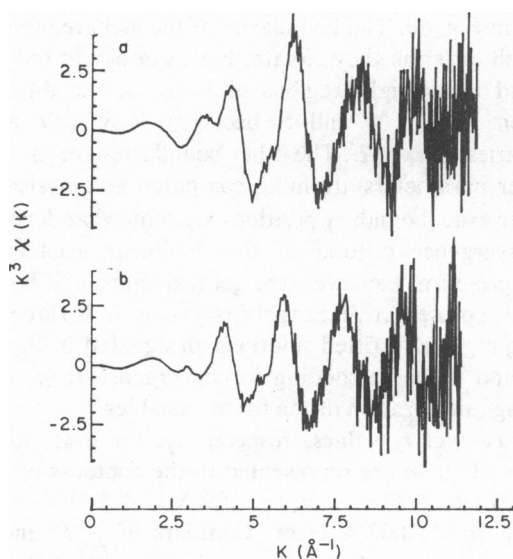


FIGURE 2 Background removed or total EXAFS data multiplied by k^3 for (a) oxidized and (b) reduced stellacyanin.

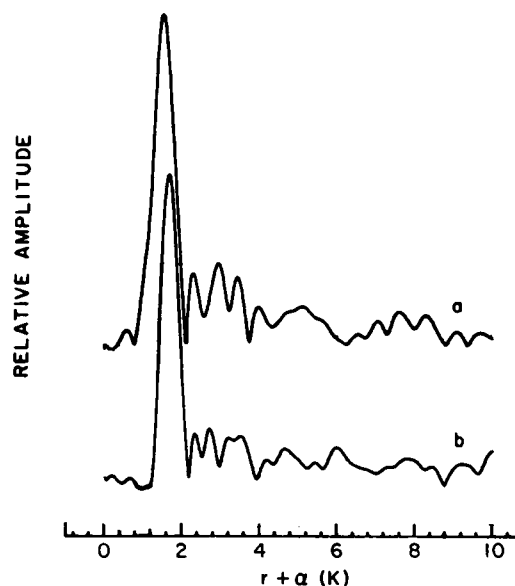


FIGURE 3 Fourier-transformed data for (a) oxidized and (b) reduced stellacyanin. Note that the abscissa contains the phase $\alpha(k)$.

Cu(II)-diethyldithiocarbamate (Cudtc), which has four sulfur atoms at an average distance of 2.316 \AA (30, 31). The fitting program used to compare the models with back-transformed data is described by Brown et al. (32). The variable parameters for each of the two atom types, denoted by subscripts N and S, are r , the average distance from the copper atom; N , the number of atoms at this average distance; $\Delta\sigma^2$, the change in disorder contribution with respect to the model; and ΔE_0 , the change in edge or threshold energy with respect to that chosen for the model. The sum of the residuals squared, $\sum R_i^2$, is useful when comparing different fits having the same input data. The parameters are not orthogonal; the largest correlations are generally found between N and $\Delta\sigma^2$. Standard analytical methods were used to determine these correlations and the directions of largest change.

The fitting algorithm was applied in a novel way that gave us increased insight into the mathematical behavior of this complicated analytical problem. The solution was considered to consist of nitrogen and/or sulfur atoms as copper ligands exclusively. The two parameters related to N_N and N_S were held fixed and the other six were permitted to vary so as to find a minimum $\sum R_i^2$, a procedure that is always at least locally convergent. For each such mathematical solution, a decision was made as to whether it was physically acceptable or not (criteria are discussed

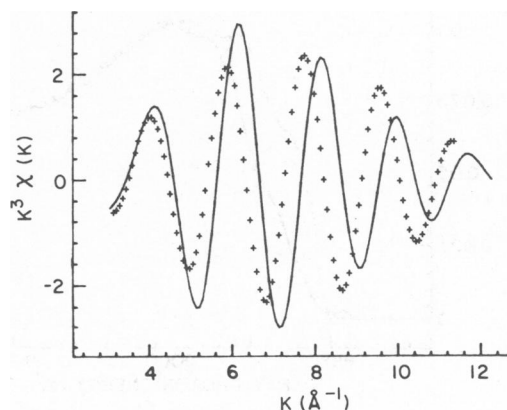


FIGURE 4 First-shell filtered data of oxidized (—) and reduced (+) stellacyanin.

below). Then a locus containing all physically acceptable solutions could be circumscribed about all such points. Then the six variable parameters were set to widely differing initial values to search for alternative local minima. A well-conditioned data set will have one such minimum (a global one), but arbitrary data may have as many minima as are permitted by the number of degrees of freedom in the data.

RESULTS

X-ray Absorption Edge Data

The structural features of the absorption edge contain information about the molecular energy levels of the absorbing atom. The systematics of these structural features have been reported elsewhere for copper model compounds and proteins (26). Fig. 5 compares the edges of oxidized and reduced stellacyanin.

The oxidized protein displays a $1s \rightarrow 3d$ transition that is expected for most Cu(II) compounds. As discussed previously (26, 28, 33), the observation of this transition clearly identifies a Cu(II) or Cu(III) oxidation state. The $1s \rightarrow 4p$ transition region is resolved into three transitions having energy differences of ~ 3 and ~ 6 eV, respectively, indicating $p_x \neq p_y \neq p_z$. This is typical of distorted tetragonal (or distorted tetrahedral) coordination. In addition, a shoulder is observed between the $1s \rightarrow 3d$ and $1s \rightarrow 4p$ transitions that is likely a $1s \rightarrow 4s$ transition. This latter is classically "forbidden" but lack of inversion symmetry can cause its appearance (32).

Upon reduction of the protein, the $1s \rightarrow 3d$ transition is not observed, as expected for Cu(I). The $1s \rightarrow 4p$ transition region is resolved into two transitions having an energy difference of ~ 7 eV, indicating $p_z < p_x \approx p_y$. This is indicative of trigonal or tetragonal geometry. However, the $1s \rightarrow 4s$ transition would not be as prominent for tetragonal geometry as for trigonal symmetry, which suggests that the latter is most likely to occur for the reduced protein.

Not until these edge features are completely understood in terms of molecular orbitals or the site structure is modeled by well-characterized compounds can they be

used to identify unambiguously the chemical type of ligands.

EXAFS Data

Oxidized state. It is complicated to fit the first-shell-filtered stellacyanin data to nitrogen and sulfur, the probable ligands, because the difference in average distance of the nitrogen and sulfur ligands to the copper atom is too small for each contribution to be resolved in the data (i.e., the first shell peaks in the Fourier transforms are single peaks and the filtered data of these contain no beat nodes). The parameters N and $\Delta\sigma^2$ are highly correlated for each type of ligand atom, and, in addition, the amplitudes for nitrogen and sulfur are similar enough so that reasonable changes in $\Delta\sigma^2$ make them difficult to distinguish. For these reasons, the EXAFS technique cannot uniquely discriminate their respective contributions.

Values of $\Delta\sigma^2$, for which $-6 \times 10^{-3} \text{ \AA} \leq \Delta\sigma^2 \leq 6 \times 10^{-3} \text{ \AA}$, are considered physically acceptable since $\Delta\sigma$ for liquids is $\sim 0.1 \text{ \AA}$. Values of ΔE_0 were restricted so that the threshold energies for nitrogen and sulfur differed by no more than 16.5 eV. This number is conservative and somewhat arbitrary but is based on the largest difference in E_0 found in our studies of copper model compounds (26). If this difference is larger than ± 2 eV, the approximation that ΔE_0 is small in the fitting program is not valid, and this parameter becomes significantly correlated to other parameters. When this occurs, the E_0 used in the analysis of the model is appropriately changed by a few electronvolts, and the fitting program is rerun. Solutions could be arbitrarily declared physically unacceptable based on very long or very short metal-ligand distances, but that situation did not arise in these calculations.

As described in Methods, loci of all physically acceptable mathematical solutions were constructed and are shown in Fig. 6a. The boundaries of the loci are labeled as to which criterion they violate. For example, in the upper left and lower right regions of locus A, the difference between E_0 for N and S becomes > 16.5 eV at the boundaries marked E. The other boundaries are caused by disorder parameters attaining computed nonphysical values. The exact boundary positions are somewhat dependent on convergence criteria of the nonlinear least-squares fitting program. However, the general shape and boundaries are representative. Surprisingly, one finds three overlapping regions of fitted solutions, designated in Fig. 6 as A, B, and C, corresponding to convergence from widely differing initialization of the fitted variables.

The r_N and r_S values, respectively, for each solution region of Fig. 6a are represented in the contours of loci B and C where $1.90 \text{ \AA} \leq r_N \leq 1.99 \text{ \AA}$ and $2.11 \text{ \AA} \leq r_S \leq 2.22 \text{ \AA}$, with $\pm 0.02 \text{ \AA}$ error. Contours of $\sum R_i^2$ indicate that solution region C is not as good as those of A and B by at least a factor of 2. Five solutions having integer values of N_N and N_S are contained in region A. The fit parameters

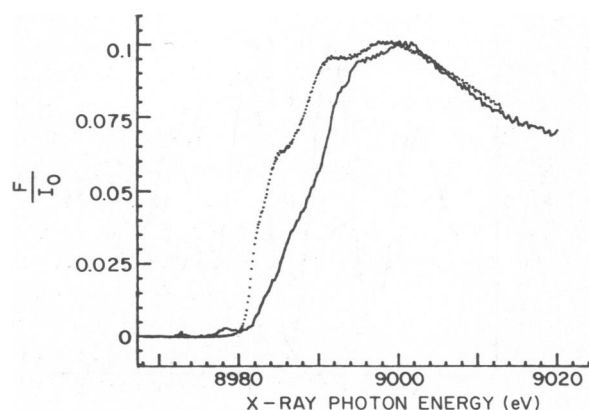


FIGURE 5 X-ray absorption edge spectra of oxidized (—) and reduced (· · ·) stellacyanin. A linear background has been subtracted to set the absorption below the first transition equal to zero.

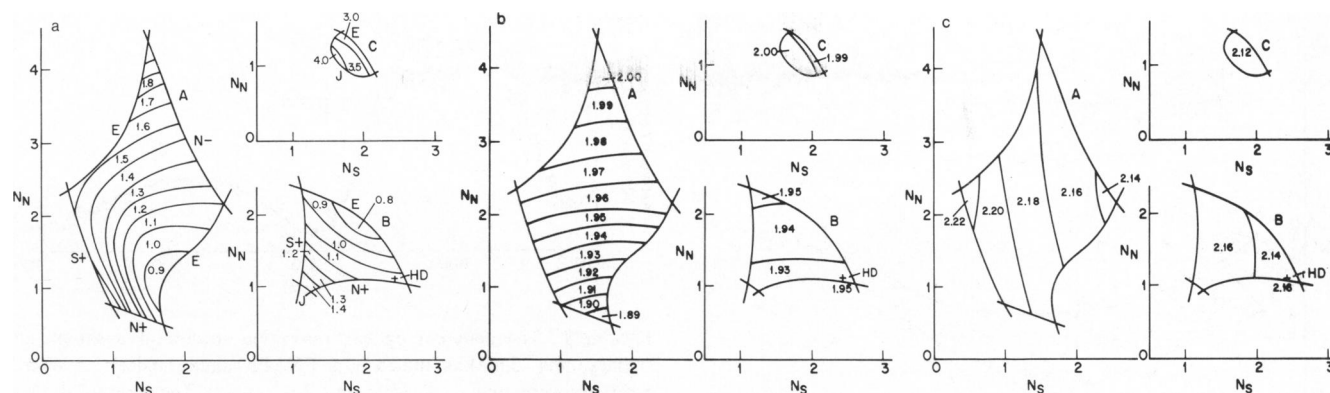


FIGURE 6 Mathematical solutions to the EXAFS equation returned by the nonlinear fitting program for oxidized stellacyanin. (a) Three loci of physically acceptable solutions, A, B, and C. The boundaries are denoted by N_{\pm} or S_{\pm} , indicating that the disorder parameter for N or S has become too large or too small (range $\pm 6 \times 10^{-3}$ from models) and by E, indicating that the threshold energies of N and S differed too greatly. J indicates an unstable jump to a more favorable solution. Note that the loci A, B, and C partially overlap the same region of parameter space. Contours show levels of equal ΣR_i^2 . (b) Loci showing levels of equal Cu—N distance. (c) Loci showing levels of equal Cu—S distance.

for these five solutions are given in Table I and will be individually discussed below.

Reduced State. For reduced stellacyanin, there is the same ambiguity in the assignment of chemical type and number of ligands as for the oxidized protein. Fig. 7 shows these results. Four solution regions (A, B, C, and D) are distinguished, but only B and C contain both nitrogen and sulfur ligands. Regions A and D are actually line segments that describe only nitrogen or only sulfur ligation, respectively. Although $\sum R_i^2$ is larger for A than for B or C, A contains only one-half the number of parameters, making it somewhat comparable to regions B and C in "goodness of fit." Solution D may be discarded on the basis of its poor fit. Within region B three solutions having integer values of N_N and N_S are found, and their fit parameters are summarized in Table I.

Radiation Damage. The effects of x-rays on oxidized stellacyanin at temperatures between 25° and –50°C were monitored optically before, during, and after the EXAFS experiment. As indicated previously (24), x-rays produce hydrated electrons so that it was thought

that reduction might take place. For a 1-mM sample of protein, loss of color was observable at a rate as high as 0.25%/s at room temperature. Fig. 8 shows that the color loss that occurs at –50°C after irradiation for the time required for four scans (a total of 28 min) is 7% of that of the native state. However, the x-ray edge of this partially bleached sample is not significantly shifted to lower energy, suggesting that color loss takes place without chemical reduction of Cu(II), but arises from a loss of integrity of the blue copper site. At temperatures below –100°C we find that color loss is greatly diminished so that samples may be studied for 4 h without a detectable change of optical properties. Under these conditions trapped radicals observed by EPR (24) accumulate to approximately the sample concentration (1 mM) with no obvious damage. Nevertheless, the two monitoring methods are used continuously and periodically, respectively, to ensure that sample changes of $> \sim 10\%$ did not occur. A cautionary warning arises from these studies. A sample irradiated at –100°C for 2 h at $\sim 10^{10}$ photons/s was warmed to the melting point, whereupon the accumulated trapped radicals drastically altered the protein, as indicated by optical bleaching and presumably by other reactions as well.

The effects of radiation at temperatures between 25° and –50°C are also reflected in EXAFS data that were collected after the sample showed no further changes with time when in the x-ray beam. The EXAFS data, $k^3\chi(k)$, and Fourier transforms are shown in Figs. 9 and 10 for stellacyanin that was initially oxidized or reduced before radiation exposure at these temperatures. Fig. 11 compares the first-shell-filtered data with that collected at temperatures of –140°C or below (cf. Fig. 4), where it was shown optically that there was little or no change on radiation exposure. The increase of amplitudes in Fig. 11 suggests that the radiation-damaged oxidized protein contains an extra ligand, probably sulfur. However, there are only small changes in the average distances to each of the ligand atoms. Analysis similar to that described above

TABLE I
FIT PARAMETERS FOR THE PHYSICALLY ACCEPTABLE
SOLUTIONS TO THE EXAFS OF OXIDIZED (ox) AND
REDUCED (re) STELLACYANIN

Solution	r_N	r_S	$\Delta\sigma_N^2$	$\Delta\sigma_S^2$	ΔE_0	ΣR_i^2
ox1N1S	1.92	2.20	4.3×10^{-3}	5.0×10^{-3}	0.1	1.41
ox2N1S	1.96	2.21	-0.8×10^{-3}	1.5×10^{-3}	0.4	1.40
ox3N1S	1.99	2.21	-3.1×10^{-3}	-1.2×10^{-3}	-0.2	1.78
ox2N2S	1.96	2.18	-3.4×10^{-3}	-1.8×10^{-3}	-3.1	1.32
ox3N2S	1.99	2.17	-4.5×10^{-3}	-3.3×10^{-3}	-1.1	1.76
re2N0S	2.10	—	3.0×10^{-3}	—	—	1.28
re1N1S	2.07	2.31	5.6×10^{-3}	-0.1×10^{-3}	1.2	0.59
re1N2S	2.07	2.26	5.1×10^{-3}	-6.2×10^{-3}	3.3	0.82
re1N3S	2.06	2.22	4.9×10^{-3}	-7.8×10^{-3}	2.6	0.90

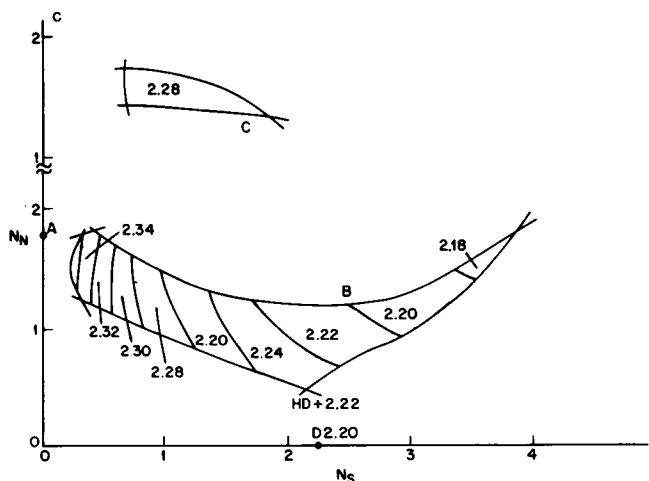
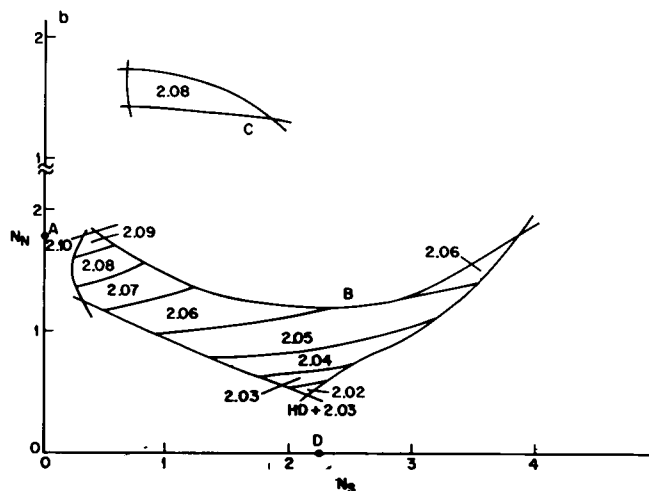
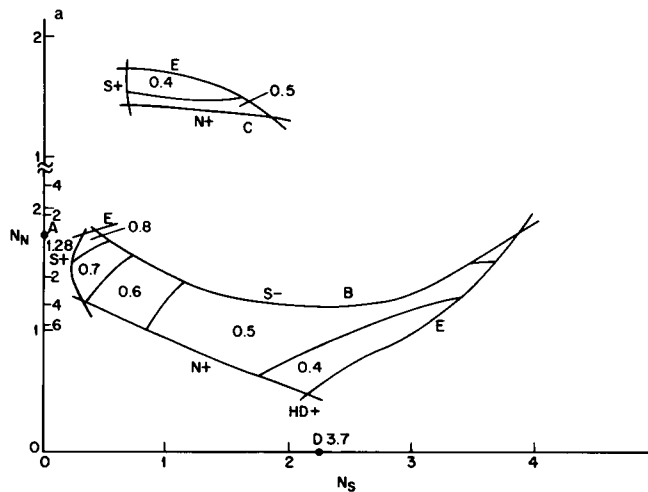


FIGURE 7 Mathematical solutions to the EXAFS equation returned by the nonlinear fitting program for reduced stellacyanin. (a) Loci of physically acceptable solutions. The boundaries are denoted as in Fig. 6a. (b) Loci showing levels of equal Cu—N distance. (c) Loci showing levels of equal Cu—S distance.

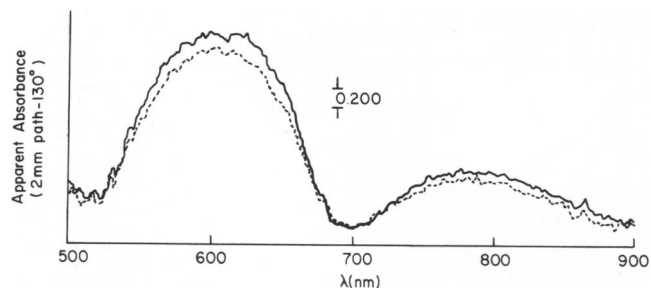


FIGURE 8 The apparent optical absorption spectra of a sample of stellacyanin (~ 3 mM as studied in the EXAFS sample holder): —, before x-ray exposure; and ···, after four 7-min scans. Temperature during irradiation was -50°C and optical spectra were recorded at -130°C with 2-mm optical path.

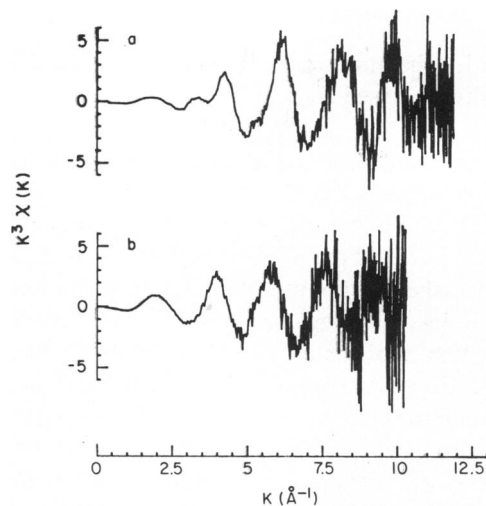


FIGURE 9 Total EXAFS spectra (with background subtracted) multiplied by k^3 of the radiation-damaged stellacyanin in (a) the oxidized and (b) the reduced states.

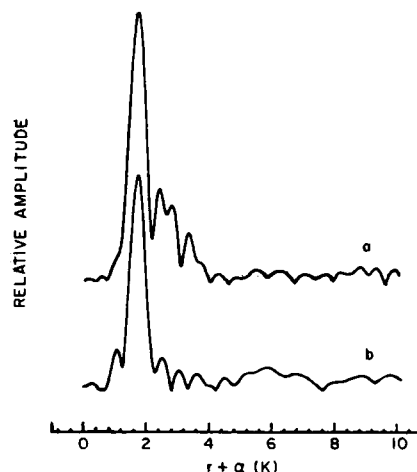


FIGURE 10 Fourier-transformed data of radiation-damaged (a) oxidized and (b) reduced stellacyanin.

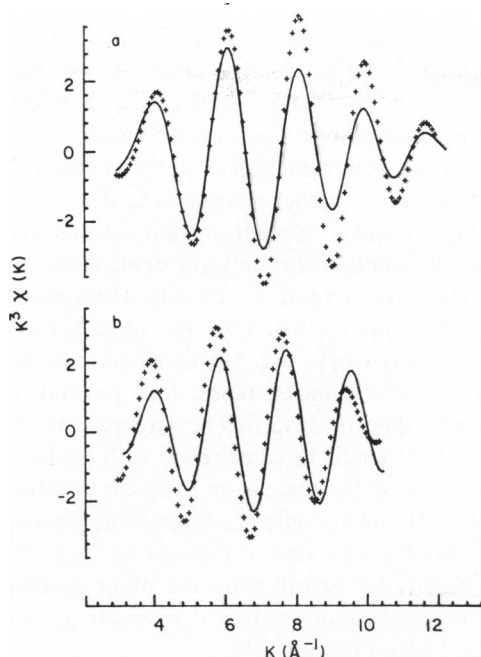


FIGURE 11 First-shell filtered data of (a) oxidized (—) and radiation-damaged oxidized (+) and (b) reduced (—) and radiation-damaged reduced (+) stellacyanin.

confirm that this is the case, with $N_N = 2$, $r_N = 1.99 \text{ \AA}$, $N_S = 2$, $r_S = 2.16 \text{ \AA}$. Similarly, it appears from Fig. 11 that an additional ligand is present in the radiation-damaged reduced protein, which in this case is probably a nitrogen atom, and that the average ligand distance is now larger. In fact, analysis shows $N_N = 2$, $r_N = 2.08 \text{ \AA}$ with $N_S = 2$, $r_S = 2.31 \text{ \AA}$. The distance error in both redox states is $\pm 0.03 \text{ \AA}$. The ligand distances in neither redox state of damaged stellacyanin are similar to those found in undamaged reduced stellacyanin or in either of the reduced states reported for plastocyanin (15, 34) as might have been expected if reduction by hydrated electrons were the only process to have occurred. Previously, Chance et al. (24) reported similar observations with cytochrome *c* oxidase; reduction by hydrated electrons takes place, accompanied by structural changes unlike those caused by chemical reduction.

Fig. 12 compares x-ray edge absorption data for radiation-damaged protein with those for the undamaged protein (Fig. 5). The data for damaged and undamaged oxidized proteins are nearly identical with the only differences being a shift of $\sim 1 \text{ eV}$ of the $1s \rightarrow 3d$ transition to lower energy and a loss of resolution in the $1s \rightarrow 4s$ region. For the oxidized damaged protein, the structural change that takes place (probably the addition of a second sulfur atom to the first coordination shell at the same distance as the original one) apparently alters the geometry of the copper site only slightly.

DISCUSSION

The five mathematically and physically acceptable solutions with integral values of N_N and N_S for oxidized

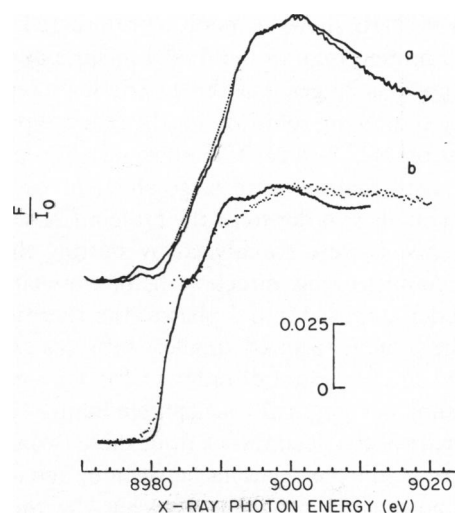


FIGURE 12 X-ray absorption edge data of (a) oxidized (—) and damaged oxidized (· · ·) and (b) reduced (—) and damaged reduced (· · ·) stellacyanin. A linear background has been removed to set the absorption below the first transition equal to zero.

stellacyanin and the four acceptable solutions for reduced stellacyanin will be discussed individually. The values of the parameters of the fit of each are listed in Table I.

Solution ox1N1S has the physical disadvantage that, with only two ligands, the x-ray edge and EPR spectra would be difficult to explain. As noted above, the x-ray edge suggests centrosymmetry; the EPR spectrum is rhombic and is unlikely to arise from bidentate coordination. Also, two-atom coordination implies a most unusual chemistry for Cu(II), which in most instances is found with four near ligands.

Solution ox2N1S has the disorder parameters that one would expect, relative to the model compounds. The Cu—N distance is slightly longer than in the model and slightly more disordered; the Cu—S distance is shorter than the model and more ordered. The three near ligands would be somewhat analogous to the copper site in oxidized plastocyanin and azurin and could give rise to the observed x-ray edge and EPR spectra.

Solution ox3N1S has a more disordered Cu—S bond than the model, although its length is shorter. The fit is not as good as that for ox2N1S. While, in principle, one sulfur atom could be formally S^- with the other S^0 , this would lead to a very large disparity in Cu—S distances, which would appear as a greatly disordered metal-ligand bond.

Solution ox3N2S provides for more disorder in both the Cu—N and Cu—S bonds than in the models. Five close neighbors to Cu(II) is an unusual situation except in porphyrins and in square pyramidal complexes supported by macrocycles. The fit is not as good as that for ox2N1S.

Solution re2N0S provides the worst fit of the various plausible solutions for the reduced protein, but as there are few variable fitting parameters, this is not so disadvantageous as it may first seem, and we cannot discount this solution entirely.

Solution re1N1S shows a much more ordered Cu—N bond in the protein than in the model in spite of the fact that its distance is longer, but this puzzle is present in all three sulfur-containing solutions for the reduced protein.

Solutions re1N2S and re1N3S show disordered Cu—S bonds and both require quite large shifts in ΔE_0 of the model compounds in order to fit the protein EXAFS data. When the models were reanalyzed by shifting their own ΔE_0 in a compensating direction before preparing the derived model amplitudes and phases, the resulting solutions for the protein required smaller shifts (as expected) but resulted in even more disorder in the Cu—S bonds, even exceeding our physically acceptable limits. This indicates that part of the goodness of fit of these two solutions may be attributed to correlations between E_0 and σ^2 rather than to a good correspondence between the theoretical model and the molecule. If either of these solutions is chosen to represent that for the reduced protein, it would be suggestive that the sulfur atoms are quite inequivalent, even though they are all in the first coordination sphere.

In summary, the ox2N1S solution seems the most favorable for the oxidized protein but not by an overwhelmingly convincing margin. For the reduced state, one can say that the metal site most likely contains only one nitrogen atom and very possibly only one sulfur atom. If there is more than one sulfur atom present, then they must be quite inequivalent to provide the observed disorder.

Relationship to Other Structural Parameters. Recently, the crystal structure of reduced plastocyanin has been reported and a high and a low pH form found (34). The high pH or redox active form contains one sulfur (2.2 Å) and two nitrogen atoms (2.1, 2.3 Å) in the first coordination shell of the copper atom with the methionine sulfur at a longer distance (2.9 Å). The low pH or protonated form contains one nitrogen and two sulfur atoms (one of which is the methionine sulfur) in the first shell with the second nitrogen suggested to be protonated and at a longer distance (3.3 Å). This structure has a trigonal geometry and has ligand distances similar to those found for the $N_N = 1$ and $N_S = 2$ solution for the EXAFS data of stellacyanin when account is taken of the fact that the average distance found by the EXAFS technique is a r^{-2} average.

As mentioned earlier, stellacyanin contains no methionine, as do plastocyanin and azurin. The methionyl sulfur to copper distance is long in oxidized plastocyanin (15) and azurin (18), 2.90 Å. Higher coordination shells are observed in Fig. 3, and an attempt was made to analyze the EXAFS data so as to determine the nature of the atoms in these shells. The second shell contribution for stellacyanin was therefore examined by making a phase comparison with the first coordination shell of CuTPP, which contains N, the fourth shell of CuTPP, which contains C, the first shell of CuO, which contains O and the first shell of Cudtc which contains S. The best comparison was with Cudtc,

giving an average distance of 2.82 ± 0.03 Å, but, the fourth shell of CuTPP was also a likely candidate, giving an average distance of 2.95 ± 0.03 Å. The possibility that this shell is a sum of contributions from different atoms is likely, but without information as to the chemical types of contributing atoms, further analysis is futile.

Both Figs. 6 and 7 contain a point labeled HD. This designates the solutions for both the oxidized and reduced proteins that are arrived at by the Hodgson-Doniach method (35). This method uses the total EXAFS data (similar to that shown in Fig. 2) which contains the sum of contributions of all shells, noise, and possibly residual contributions due to insufficient background removal. These data are then fit by comparison with models, and no change is allowed for the $\Delta\sigma^2$ or ΔE_0 contributions (i.e., $\Delta\sigma^2 = \Delta E_0 = 0$). The problems and possible pitfalls of this approach are demonstrated in Figs. 6 and 7 together with reported results for azurin (36) and other proteins (37). Detailed discussions of analytical methods are given by Lee et al. (27) and Powers (28).

That portion of this work carried out at the Albert Einstein College of Medicine was supported by a U.S. Public Health Service grant HL-13399 to Dr. Peisach and as such is Communication 423 from the Joan and Lester Avnet Institute of Molecular Biology. Part of this work was done at the Stanford Synchrotron Radiation Laboratory under Proposal No. 105/423 and 424. The portion of this work carried out at the University of Pennsylvania was supported in part by U.S. Public Health Service grants GM-27308, GM-28385, HL-15061, and HL-18708 to Dr. B. Chance.

Received for publication 2 October 1981 and in revised form 8 January 1982.

REFERENCES

1. Malkin, R., B. G. Malmström. 1970. The state and function of copper in biological systems. *Adv. Enzymol.* 33:177-244.
2. Fee, J. A. 1975. Copper proteins: systems containing the "blue" copper center. *Struct. Bonding.* 23:1-60.
3. McMillan, D. R., R. C. Rosenberg, and H. B. Gray. 1974. Preparation and spectroscopic studies of cobalt(II) derivatives of blue copper proteins. *Proc. Natl. Acad. Sci. U.S.A.* 71:4760-4762.
4. Solomon, E. I., J. W. Hare, and H. B. Gray. 1976. Spectroscopic studies and a structural model for blue copper centers in proteins. *Proc. Natl. Acad. Sci. U.S.A.* 73:1389-1393.
5. Peisach, J., W. G. Levine, and W. E. Blumberg. 1967. Structural properties of stellacyanin, a copper mucoprotein from *Rhus vernicifera*, the Japanese lac tree. *J. Biol. Chem.* 242:2847-2858.
6. Markley, J. L., E. L. Ulrich, S. P. Berg, and D. W. Krogman. 1975. Nuclear magnetic resonance studies of copper binding sites of blue copper proteins: oxidized, reduced and apoplastocyanin. *Biochemistry.* 14:4428-4433.
7. Ugurbil, K., A. Norton, A. Allerhand, and R. Bersohn. 1977. Studies of individual carbon sites of Azurin from *Pseudomonas aeruginosa* by natural abundance carbon-13 nuclear magnetic resonance spectroscopy. *Biochemistry.* 16:886-894.
8. Hill, H. A. O., and L. Wing-Kai. 1979. Investigation of the structure of the blue copper protein from *Rhus vernicifera*, stellacyanin, by proton magnetic resonance spectroscopy. *J. Inorg. Biochem.* 11:101-113.
9. Mims, W. B., and J. Peisach. 1976. Assignment of a ligand in stellacyanin by a pulsed electron paramagnetic resonance method. *Biochemistry.* 15:3863-3868.

10. Mims, W. B., and J. Peisach. 1979. Measurement of ^{14}N superhyperfine frequencies in stellacyanin by an electron spin echo method. *J. Biol. Chem.* 254:4321–4323.
11. Roberts, J. E., T. G. Brown, B. M. Hoffman, and J. Peisach. 1980. Electron-nuclear double resonance spectra of stellacyanin. *J. Am. Chem. Soc.* 102:825–829.
12. Peisach, J., and W. B. Mims. 1978. The linear electric field effect in stellacyanin, azurin, and in some simple model compounds. *Eur. J. Biochem.* 84:207–214.
13. Sugiura, Y., Y. Hirayama, H. Tanaka, and K. Ishizu. 1975. Copper (II) complexes of sulfur-containing peptides. Characterization and similarity of electron spin resonance spectrum to the chromophore in blue copper proteins. *J. Am. Chem. Soc.* 97:5577–5581.
14. Thompson, J. S., T. J. Marks, and J. A. Ibers. 1977. Blue copper proteins: synthesis, spectra, and structures of $\text{Cu(I)N}_3(\text{SR})$ and $\text{Cu(II)N}_3(\text{SR})$ active site analogs. *Proc. Natl. Acad. Sci. U.S.A.* 74:3114–3118.
15. Colman, P. M., H. C. Freeman, J. M. Guss, M. Murata, V. A. Norris, J. A. M. Ramshaw, and M. P. Venkatappa. 1978. X-ray crystal structure analysis of plastocyanin at 2.7 Å resolution. *Nature (Lond.)* 272:319–324.
16. Blumberg, W. E., and J. Peisach. 1966. The optical and magnetic properties of copper in *Chenopodium album* plastocyanin. *Biochim. Biophys. Acta.* 126:269–273.
17. Sailasuta, N., F. C. Anson, and H. B. Gray. 1979. Studies of the thermodynamics of electron transfer reactions of blue copper proteins. *J. Am. Chem. Soc.* 101:455–458.
18. Adman, E. T., R. E. Stenkamp, L. C. Sieker, and L. H. Jensen. 1978. A crystallographic model for azurin at 3 Å resolution. *J. Mol. Biol.* 123:35–48.
19. Miskowski, V., S.-P. Tang, T. G. Spiro, E. Shapiro, and T. H. Moss. 1975. The copper coordination in "blue" copper proteins: evidence from resonance Raman spectra. *Biochemistry.* 14:1244–1250.
20. Omura, T. 1961. Studies on laccase of lacquer trees IV. Purification and properties of a blue protein obtained from latex of *Rhus vernicifera*. *J. Biochem., (Tokyo).* 50:395–399.
21. Malmström, B. G., B. Reinhammar, and T. Vänngård. 1970. The state of copper in stellacyanin and laccase from the lacquer tree *Rhus vernicifera*. *Biochim. Biophys. Acta.* 205:48–57.
22. Brill, A. S., G. F. Bryce, and H. J. Maria. 1968. Optical and magnetic properties of *Pseudomonas* azurins. *Biochim. Biophys. Acta.* 154:342–351.
23. Bergman, C., E. K. Gandvik, P. O. Nyman, and L. Strid. 1977. The amino acid sequence of stellacyanin from the lacquer tree. *Biochem. Biophys. Res. Commun.* 77:1052–1059.
24. Chance, B., P. Angiolillo, E. K. Yang, and L. Powers. 1980. Identification and assay of synchrotron radiation induced alterations on metalloenzymes and proteins. *FEBS (Fed. Eur. Biochem. Soc.) Lett.* 112:178–182.
25. Powers, L., B. Chance, Y. Ching, and P. Angiolillo. 1981. Structural features and the reaction mechanism of cytochrome oxidase: iron and copper x-ray absorption fine structure. *Biophys. J.* 34:465–498.
26. Powers, L., W. E. Blumberg, B. Chance, C. H. Barlow, J. S. Leigh, Jr., J. Smith, T. Yonetani, S. Vik, and J. Peisach. 1979. The nature of the copper atoms of cytochrome *c* oxidase as studied by optical and x-ray absorption edge spectroscopy. *Biochim. Biophys. Acta.* 546:520–538.
27. Lee, P. A., P. H. Citrin, P. Eisenberger, and B. M. Kincaid. 1981. Extended x-ray absorption fine structure, its strengths and limitations as a structural tool. *Rev. Mod. Phys.* 53:769–806.
28. Powers, L. 1982. X-ray absorption spectroscopy: application to biological molecules. *Biochim. Biophys. Acta.* In press.
29. Fleischer, E. B., C. K. Miller, and L. E. Webb. 1964. Crystal and molecular structures of some metal tetraphenylporphines. *J. Am. Chem. Soc.* 86:2342–2347.
30. Reddy, T. R., and R. Srinivasan. 1965. EPR and optical studies in copper diethyldithiocarbamate. *J. Chem. Phys.* 43:1404–1409.
31. O'Connor, B. H., and E. N. Maslen. 1966. A second analysis of the crystal structure of copper(II) diethyldithiocarbamate. *Acta Crystallogr.* 21:828–830.
32. Brown, J. M., L. Powers, B. Kincaid, J. A. Larrabee, and T. G. Spiro. 1980. Structural studies of the hemocyanin active site. I. Extended x-ray absorption fine structure (EXAFS) analysis. *J. Am. Chem. Soc.* 102:4210–4216.
33. Blumberg, W. E., J. Peisach, and D. J. Kosman. 1982. Is Cu(III) a viable oxidation state in biological systems? In *Oxidases and Related Redox Systems*. M. Morrison, H. S. Mason, and T. E. King, editors. University Park Press, Baltimore. In press.
34. Freeman, H. C. 1981. Electron transfer in "blue copper proteins." In *Proceedings of XXI International Conference on Coordination Chemistry*. Pergamon Press, New York. In press.
35. Cramer, S. P., K. O. Hodgson, E. I. Stiefel, and W. F. Newton. 1978. A systematic x-ray absorption study of molybdenum complexes. The accuracy of structural information from extended x-ray absorption fine structure. *J. Am. Chem. Soc.* 100:2748–2760.
36. Tullius, T. D., P. Frank, and K. O. Hodgson. 1978. Characterization of the blue copper site in oxidized azurin by extended x-ray absorption fine structure: Determination of a short Cu-S distance. *Proc. Natl. Acad. Sci. U.S.A.* 75:4069–4073.
37. Cramer, S. P., J. H. Dawson, K. O. Hodgson, and L. P. Hager. 1978. Studies on the ferric form of cytochrome *P-450* and chloroperoxidase by extended x-ray absorption fine structure. Characterization of the Fe—N and Fe—S distances. *J. Am. Chem. Soc.* 100:7282–7290.